0026-895X/99/050873-10$3.00/0

MOLECULAR PHARMACOLOGY, **55:**873–882 (1999).

Functional Roles of Aromatic Residues in the Ligand-Binding Domain of Cyclic Nucleotide-Gated Channels

JUN LI[1] and HENRY A. LESTER

Division of Biology, California Institute of Technology, Pasadena, California

Received June 2, 1998; accepted December 30, 1998.

This paper is available online at http://www.molpharm.org

ABSTRACT

The ligand-binding domains of cyclic nucleotide-gated (CNG) channels show sequence homology to corresponding region(s) of the *Escherichia coli* catabolite gene-activator protein (CAP) and to the regulatory subunit of cAMP-dependent or cGMP-dependent protein kinases. The structure of CAP and that of a cAMP-dependent protein kinases regulatory subunit have been solved, prompting efforts to generate structural models for the binding domains in CNG channel. These models explicitly predicted that an aromatic residue in the CNG channel aligning with leucine 61 of CAP forms an interaction with the bound cyclic nucleotide. We tested this hypothesis by site-directed mutagenesis in a rat olfactory channel (rOCNC1) and a bovine rod photoreceptor channel (Brcng). We found that mutations at this site had only weak effects that were not specific to the aromatic or the hydrophobic nature of the substituted residue. This result weakens the hypothesis of a strong or specific interaction at this site. We also separately mutated most of the other aromatic residues in the binding domain to alanine; most of these mutations resulted in channels that either did not function or had only minor changes in sensitivity. However, replacing tyrosine 565 with alanine (Y565A) in rOCNC1 increased agonist sensitivity by ~10-fold and resulted in prominent spontaneous activities. Y565 presumably lies between two α helices in the binding domain; one of these, the C helix, probably rotates during channel activation. The position of Y565 at the "hinge" between the C helix and another portion of the binding domain, and the consequences of Y565 mutations, strongly suggest that this portion of the binding domain is involved in channel gating processes.

Cyclic nucleotide-gated (CNG) channels are plasma membrane cation channels directly activated by cytoplasmic cAMP or cGMP (Fesenko et al., 1985; Nakamura and Gold, 1987). They play important roles in visual (Yau and Baylor, 1989) and olfactory (Zufall et al., 1994) signal transduction. For every cloned CNG channel subunit, the deduced amino acid sequence contains a "core" channel domain, followed by a carboxyl-terminal cyclic nucleotide-binding domain. Similar to voltage-gated channels, the core has six putative transmembrane segments and a P region, which constitutes part of the pore (Jan and Jan, 1990). The binding domain is homologous to the cyclic nucleotide-binding sequences conserved from the *Escherichia coli* catabolite gene-activator protein (CAP), an *E. coli* transcription regulator, to the regulatory subunits of protein kinase A (PKA) or protein kinase G (Shabb and Corbin, 1992).

The atomic structures of CAP (McKay and Steitz, 1981; Weber and Steitz, 1987) and a type 1 regulatory subunit of bovine PKA (PKA-R1) (Su et al., 1995) have been solved. In both proteins, each binding site consists of three α-helices and a distinctive eight-strand, antiparallel β-barrel. The availability of these structures allowed the use of homology modeling to construct tertiary structures of binding domains in CNG channels and to predict some important ligand-protein contact points (Kumar and Weber, 1992; Scott et al., 1996).

An early site-directed mutagenesis study identified an alanine/threonine difference that partially underlies ligand discrimination in CNG channels (Altenhofen et al., 1991). However, structural predictions at several other residues have not been tested. At a position that aligns with leucine 61 (Leu61) of CAP, for example, it was predicted that the aromatic residue at this site in CNG channels would form an important contact with bound ligand (Kumar and Weber, 1992; Scott et al., 1996). To test this hypothesis, we have introduced mutations at the predicted site [i.e., tyrosine 512 (Y512) in the α subunit of rat olfactory channel (rOCNC1) (Dhallan et al., 1990) and phenylalanine 533 (F533) in the α subunit of bovine rod photoreceptor channel (Brcng) (Kaupp et al., 1989; Gordon and Zagotta, 1995)]. A strong involve-

This research was supported by Grant NS11756 from the National Institutes of Health.

[1] Present address: Department of Genetics, Stanford University, 300 Pasteur Dr., M310, Stanford, CA 94305.

ABBREVIATIONS: CNG, cyclic nucleotide-gated; PKA, protein kinase A; CAP, *E. coli* catabolite gene-activator protein; rOCNC1, rat olfactory channel; Brcng, bovine rod photoreceptor channel; PKA-R1, type 1 regulatory subunit of bovine cAMP-dependent protein kinase; PCR, polymerase chain reaction.

ment of the predicted residue in either ligand binding or the conformational changes after binding (gating) would result in significant shifts in the EC_{50} values (for a review, see Li et al., 1997). Our results, reported herein, revealed shifts in the EC_{50} values of ≤2-fold, even with nonaromatic or charged residues. This calls into question the accuracy of the predictions and weakens the hypothesis that the tyrosine/phenylalanine difference at this position between the photoreceptor and the olfactory channels contributes to the fact that both cAMP and cGMP are potent agonists at the olfactory channels, whereas only cGMP can effectively open the photoreceptor channels.

In each of the two cAMP-binding domains of PKA-R1, there is a stacking interaction between an aromatic residue and the adenine ring of cAMP (Su et al., 1995), similar to the interactions predicted for CNG channels. However, the positions in PKA that align to CAP Leu61 are not involved. The residues that are involved, tryptophan 260 and tyrosine 371 (Fig. 1, bold), are situated at the extremes of the amino- and carboxyl-termini of repeat B, and project from outside back into the two binding pockets (Su et al., 1995). It is therefore worth testing whether such aromatic–aromatic interactions also make significant contributions to ligand binding in CNG channels and, if so, which one of the aromatic residues other than rOCNC1-Y512 or Brcng-F535 serves this function.

There are typically six to eight aromatic residues in a CNG-channel binding domain of ~120 amino acids. To examine their functional importance, we changed them to ala-

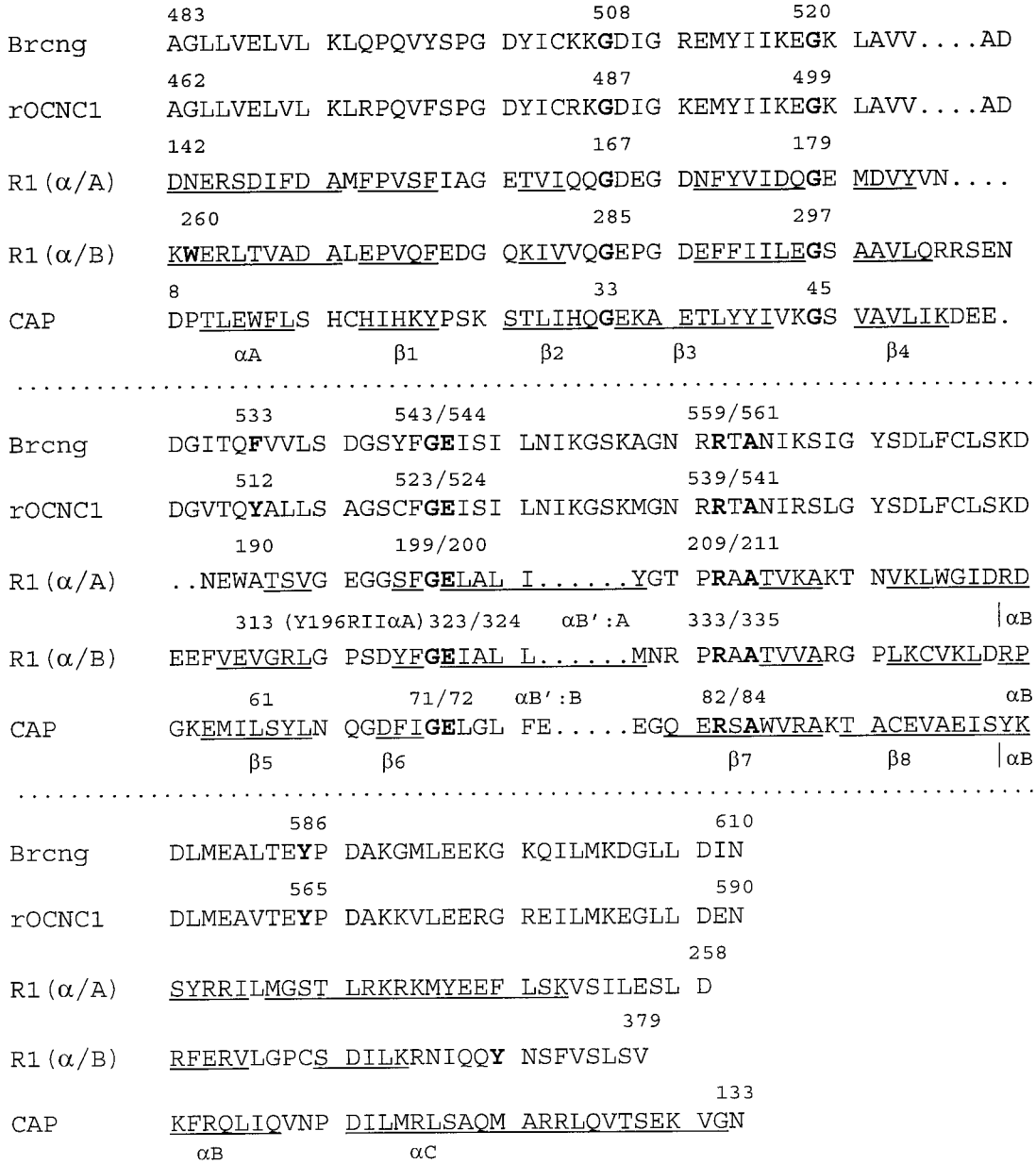

Fig. 1. Sequence alignment of cyclic nucleotide-binding domains. Shown are rOCNC1, Brcng, the two binding domains (repeat A and repeat B) in PKA R1 (α/A) and (α/B), and CAP. The six invariant residues are bold and numbered. Also highlighted are Y512 and Y565 in rOCNC1 and the aligning residues in Brcng, F533 and Y586. These two positions were studied in this project. The α helices and β strands defined in the three known structures are underlined. V193 in RI (α/A) aligns with Y196 in RII (α/A), which can be affinity labeled with cAMP analogs (Bubis and Taylor, 1987), suggesting that the bound ligand is close to this portion of the binding domain.

nine, one at a time, in the binding domain of rOCNC1. In this series of experiments, all but one aromatic residue was mutated; we expressed the mutant channels in *Xenopus laevis* oocytes and measured the dose-response relations. We also mutated some of these residues to leucine, tryptophan, glutamate, or serine. Some of the alanine mutations rendered the channel nonfunctional, whereas all but one of the functional mutants had only minor shifts in sensitivity. The interesting exception, Y565A in rOCNC1, showed 10-fold greater sensitivity to both cAMP and cGMP. The effect is caused, at least in part, by facilitated gating transitions, as indicated by the prominent spontaneous activities. Replacement of Y565 by other residues revealed that for the residue at this position, the function is related more to the size of its side chain than to such properties as the aromaticity or charge.

Materials and Methods

Mutagenesis. The cDNA for rOCNC1, kindly provided by Dr. K.-W. Yau (Howard Hughes Medical Institute, Johns Hopkins University School of Medicine, Baltimore, MD), was subcloned into pGEMHE (Liman et al., 1992) at the *Eco*RI and *Hin*dIII sites, between the 5′- and 3′-untranslated sequences of the *X. laevis* major β-globin gene for enhanced expression in oocytes. The cDNA for Brcng, already in pGEMHE, was kindly provided by Dr. William Zagotta (University of Washington, Seattle, WA).

Point mutations were introduced by a polymerase chain reaction (PCR) procedure, using primers that contain the desired base changes. The detailed steps have been described previously (Higuchi, 1990). Briefly, we separately generated two PCR fragments that incorporated the mutation at the tail end of the upstream fragment and the beginning of the downstream fragment. When these two primary PCR products were gel-purified, denatured, and allowed to reanneal, heteroduplexes formed by association of two fragments at the overlapping region. The recessed 3′ ends of these heteroduplexes were extended in a second, mutually primed PCR to form a full-length, double-stranded PCR product with the mutation situated in the middle. Only the rightmost and leftmost primers used in the first round of PCR were added in the second PCR, so that the full-length fragment was amplified.

The outside primers carried suitable restriction sites, so that the amplified full-length fragment was ligated back into the wild-type plasmid to substitute for the corresponding wild-type fragment. The PCR-derived cassette was confined by *Hin*dIII (1750) and *Hin*dIII (2505) in rOCNC1 and by *Nsi*I (1447) and *Sty*I (2165) in Brcng. The *Hin*d-*Hin*d fragment for rOCNC1 ligated with two possible orientations; these were distinguished by cutting with *Apa*I (2216) and *Pst*I (206 bases on the 3′ end of the insert).

The "inside" primers that contain the base mismatch were 21 to 27 bases in length, with the mismatch located in the center. For example, to make Y512D in rOCNC1, we used 5′-GTGACTCAGGATGCCTTGCTC-3′ and its complementary oligonucleotide as the middle primers. The underlined triplet, GAT, codes for D and is situated to replace the wild-type sequence, TAT, which codes for Y. Point deletions were introduced in the same way as substitutions. Most of the primers used in this study were synthesized in our laboratory using an Expedite Nucleic Acid Synthesis System (Millipore Corporation, Marlborough, MA), and purified by washing with ammonium chloride.

Standard molecular biology techniques were used for the transformation of bacteria, the extraction of plasmid DNA, and for other routine procedures. In the final plasmid, the sequence of the entire PCR-derived insert was verified to ensure that no random misincorporation took place during PCR. The sequencing used the Dye Terminator Cycle Sequencing kit and automatic sequencing (Applied Biosystems; Perkin-Elmer Corporation, Foster City, CA).

Expression. cRNA was synthesized in vitro (Ambion T7 mMESSAGE mMACHINE kit; Ambion, InC., Austin, TX) using plasmid linearized with *Pst*I as template. Stage V and VI *X. laevis* oocytes were each injected with 50 nl of cRNA, with concentrations ranging from 20 to 300 ng/μl. The oocytes were incubated in ND96 solution, containing 96 mM NaCl, 2 mM KCl, 1 mM $MgCl_2$, 1.8 mM $CaCl_2$, and 5 mM HEPES, pH 7.4. Recordings were made at room temperature from 24 to 120 h after injection. To improve the viability of oocytes, horse serum (HyClone Laboratories, Logan, UT) was added at 5% to the incubation solution (Quick et al., 1992).

Electrophysiological Recording and Analysis. All recordings were performed at room temperature from inside-out patches in symmetrical solutions containing 140 mM NaCl, 5 mM HEPES, and 0.2 mM EDTA, pH 7.4. The oocytes were stripped of the vitelline membrane as described previously (Quick et al., 1992), and membrane seals were formed in ND96. The patch was then excised by withdrawing the pipette, and excision was signaled by the flow of current through the endogenous Ca^{2+}-activated Cl^- channels. The perfusion solutions containing various concentrations of cAMP or cGMP were applied to the patch using an RSC100 rapid solution changer (Molecular Kinetics, Pullman, WA). Upon perfusion of divalent cation-free solution containing no cyclic nucleotide, the endoge-

Human Rod α	ADDGV TQ**F**VVLSDGS YFGEISILNI KGSKAGNRRT
Bovine Rod	ADDGI TQ**F**VVLSDGS YFGEISILNI KGSKAGNRRT
Mouse Rod	ADDGI TQ**F**VVLSDGS YFGEISILNI KGSKAGNRRT
Chicken Rod/Cone	ADDGI TQ**F**VVLSDGS YFGEISILNI KGSKSGNRRT
Bovine Cone/Sperm	AEDGI TQ**F**VVLGDGS YFGEISILNI KGSKSGNRRT
Bovine Olf	ADDGV TQ**Y**ALLSAGS CFGEISILNI KGSKMGNRRT
Rabbit Aorta	ADDGV TQ**Y**ALLSAGS CFGEISILNI KGSKMGNRRT
Rat Olf α	ADDGV TQ**Y**ALLSAGS CFGEISILNI KGSKMGNRRT
Rat Olf β	ADDGV TQ**Y**AVLGAGL YFGEISIINI KGNMSGNRRT
Catfish Olf	ADDGV TQ**F**ALLTAGG CFGEISILNI QGSKMGNRRT
Drosophila eye/antennae	GDDGI TV**L**ATLGAGS VFGEVSVLEI AGNRTGNRRT
Human Rod β	GPDGK SV**L**.TLKAGS VFGEISLLAV GG...GNRRT
PKA-R1	GPSD. ..... YFGEIALLM. .....NRPR

Fig. 2. Sequence alignment of a portion of the cyclic nucleotide-binding domain. Highlighted are the residues at the position homologous to Y512 in rOCNC1.

nous Ca^{2+}-activated Cl^- current disappeared, leaving a patch with a resistance of 1 to 4 GΩ. cAMP and cGMP were both obtained from Sigma Chemical Co. (St. Louis, MO).

The recording pipettes were fabricated from either filamented, borosilicate glass tubing (Corning type 7740; o.d., 1.5 mm; i.d., 0.86 mm; Sutter Instrument, Novato, CA), or unfilamented Kimax-51 borosilicate capillary tubing (type KG-33; o.d., 1.8 mm; i.d., 1.5 mm; Kimble/Konte, Vineland, NJ). The pipette tips were fire-polished using a Narishige MF-83 microforge (Narishige Scientific Instrument Lab, Tokyo, Japan). The filled pipettes had resistances of 2 to 8 MΩ.

Single-channel and macroscopic currents were recorded with an Axopatch-200A or an Axopatch-1D amplifier (Axon Instruments, Foster City, CA). For voltage-clamped, episodic recording, the 4-pole, low-pass Bessel filter on the amplifier was set to 1 kHz; the currents were recorded with CLAMPEX (Axon Instruments), using either step-voltage protocols or ramped-voltage protocols, both lasting 800 ms, with holding potential at 0 mV. The amplitudes of currents at specific voltages and agonist concentrations were measured in CLAMPFIT (Axon Instruments). Agonist-induced currents were obtained by subtracting currents recorded in the absence of agonist.

Macroscopic dose-response relations were fit to the Hill equation:

$$I = \frac{I_{max}}{1 + (EC_{50}/[A])^{n_H}}$$

I is the current recorded at agonist concentration ([A]). I_{max} is the maximal current, which is treated as a free parameter in fitting. EC_{50} is the concentration that elicits half-maximal response, and n_H is the Hill coefficient. The fitting used the Levenberg-Marquardt algorithm in Origin 5 (Microcal Software, Northampton, MA). The average values of the parameters are reported along with S.E.s.

For gap-free continuous recording of single channels, the membrane potential was held at −60 mV to prevent the openings of the endogenous stretch-activated channels. Openings of these channels

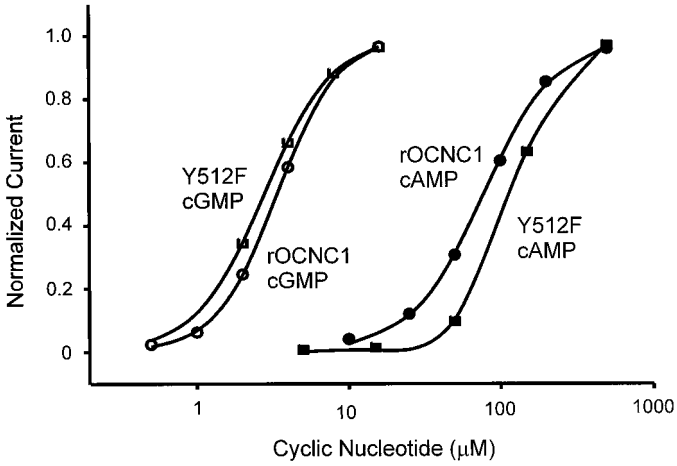

Fig. 3. Dose-response comparison between wild-type rOCNC1 and its mutant Y512F. The current responses at 80 mV were fitted to the Hill equation with I_{max}, EC_{50}, and n_H as free parameters. The current values were then normalized to I_{max} and refitted using only EC_{50} and n_H as free parameters. The horizontal axis is on a logarithmic scale.

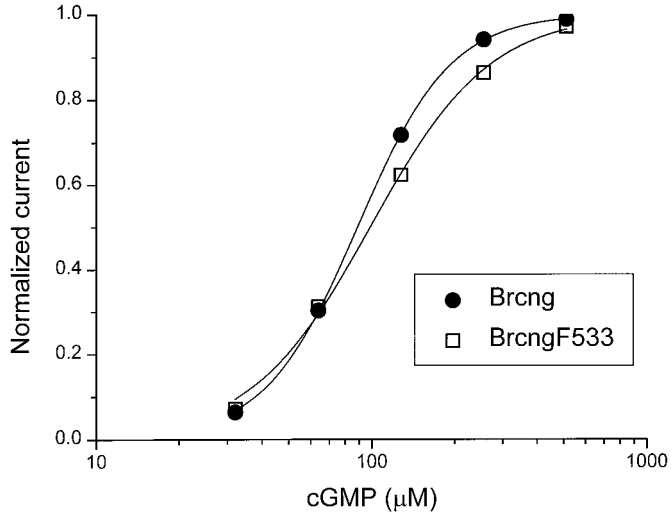

Fig. 4. Dose-response comparison between wild-type Brcng and its mutant F533Y at 80 mV. The fitting and normalization were as described in Fig. 3. The horizontal axis is on a logarithmic scale.

TABLE 1

Summary of EC_{50} and n_H values of mutants examined in this study

* For the batches of oocytes studied with the Y512A and Y512S mutants, the wild-type EC_{50} value for cAMP was 37 ± 5 μM (mean ± S.E., n = 2), rather than the usual 70 to 80 μM. Therefore, the observed cAMP EC_{50} values for Y512A and Y512S were normalized to the wild-type value of these batches.

	cAMP		cGMP	
	EC_{50} ± S.E.M. (n)	n_H ± S.E.M. (n)	EC_{50} ± S.E.M. (n)	n_H ± S.E.M. (n)
rOCNC1				
Wild-type	85 ± 7 (18)	2.0 ± 0.1 (18)	2.6 ± 0.2 (14)	2.1 ± 0.1 (14)
Y512F	188 ± 26 (6)	2.4 ± 0.1 (6)	2.8 ± 0.4 (5)	1.9 ± 0.4 (5)
Y512A	83 ± 11 (7)*	2.1 ± 0.1 (7)	1.5 ± 0.1 (2)	2.1 ± 0.2 (2)
Y512S	74 ± 18 (6)*	1.9 ± 0.1 (6)	2.7 ± 0.4 (3)	1.9 ± 0.1 (3)
Y512D	157 ± 18 (2)	1.7 ± 0.1 (2)	5.2 ± 0.2 (3)	2.3 ± 0.2 (3)
F477A	167 ± 25 (2)	1.8 ± 0.1 (2)	2.5 ± 0.9 (2)	2.0 ± 0.2 (2)
Y482W			2.9 (1)	1.4
Y547A	85 ± 40 (2)	1.8 ± 0.5 (2)	5.7 (1)	1.7
F551W			1 (1)	3.5
Y565A	9.5 ± 1.1 (10)	2.2 ± 0.3 (10)	0.33 ± 0.07 (2)	2.0 ± 0.5 (5)
Y565L	30 ± 3 (5)	2.0 ± 0.1 (5)	0.8 ± 0.1 (2)	2.1 ± 0.1 (2)
Y565D	34 ± 5 (7)	1.8 ± 0.2 (7)	1.1 ± 0.3 (5)	2.0 ± 0.2 (5)
Y565Δ	69 ± 3 (3)	2.1 ± 0.4 (3)	2.5 ± 0.6 (3)	1.5 ± 0.1 (3)
Brcng				
Wild-type			128 ± 8.7 (11)	2.2 ± 0.1 (11)
F533Y			143 ± 11 (4)	2.3 ± 0.1 (4)
F533A			126 ± 14 (4)	2.1 ± 0.1 (4)
F533D			127 ± 26 (3)	2.0 ± 0.1 (3)
Y586F			39 ± 2.0 (2)	3.4 ± 0.2 (2)
Y586W			77 ± 11 (2)	2.0 ± 0.4 (2)

n, number of measurements.

do resemble those of the rat olfactory CNG channels, but we found that the stretch-activated channels are usually inactive at −60 mV in the absence of applied suction. For each recording, we applied suction to the patch periodically to confirm either that there was no stretch-activated channel in the patch, or that such channels were inactive without suction. The Bessel filter on the amplifier was opened at its widest at 50 kHz (f_{-3dB}). The data were sampled at 44 kHz by a Neuro-Corder Digitizing Unit (model DR384; NeuroData Instruments Corp., New York, NY), and were subsequently stored on videotape. The Neuro-Corder utilizes a predigitizing, antialiasing filter with a rolloff of 70 dB within 1.5 kHz of 22 kHz (−3 dB frequency). During analysis, data were played back, converted to analog form by the Neuro-Corder, filtered at 2 kHz (corner frequency) with an 8-pole, low-pass Bessel filter (model 902; Frequency Devices Inc., Haverhill, MA), and digitized at 10 kHz with FETCHEX of PCLAMP6, via a Digidata 1200 interface (Axon Instruments). The data were idealized in FETCHAN of pCLAMP6 using half-magnitude threshold-crossing criterion for detecting event transitions. Transitions were individually inspected and manually accepted or rejected. The "P_{open} versus Elapsed time" chart and the open time- and closed time-histograms were constructed in PSTAT of PLCAMP6, and were fitted in PSTAT with sums of exponential functions using the Levenberg-Marquardt method with weighting by function. The histograms were binned with a logarithmic time axis and plotted with a square-root transformation of the vertical axis, so that the individual exponential components can be directly visualized as apparent peaks in the histograms (Sigworth and Sine, 1987).

We analyzed recordings from patches containing a single channel. This was verified by the lack of double openings during prolonged periods of activity with high open probabilities, such as P_{open}>80%.

Results

The sequence alignment shown in Fig. 1 includes the binding domains of Brcng, rOCNC1, the two tandem binding domains (repeat A and repeat B) in the splice variant α of PKA-R1 [denoted R1 (α/A) and R1 (α/B)], and CAP. In the latter three sequences, the secondary structural motifs identified in the atomic structures are underlined. These include three α-helices (αA, αB, and αC), and eight β-strands (β1 through β8). In PKA-R1, there is also an additional α helix (αB′) between β6 and β7. Highlighted in bold are the six residues absolutely conserved in the complete alignment of the more than 40 CAP-related cyclic nucleotide-binding proteins. They are at positions aligning with CAP G33, G45, G71, E72, R82, and A84.

rOCNC1-Y512F and Brcng-F533Y. Brcng F533 and rOCNC1 Y512 are also highlighted in bold in Fig. 1. They align with each other, and according to the model of Scott/Tanaka (Scott et al., 1996), a tyrosine (Y) at this position would form a strong interaction with either cAMP or cGMP, whereas a phenylalanine (F) would form only a weak interaction. In addition to this prediction, there are other reasons to study aromatic residues at this position: 1) A tyrosine in repeat A of bovine PKA-RIIα, Y196 (sequence not shown), can be affinity-labeled by cyclic nucleotide analogues (Bubis and Taylor, 1987). Y196 in PKA-RII (α/A) aligns with V193 of R1 (α/A) (the latter is shown in Fig. 1) and is near Y512 of rOCNC1. This strongly suggests a close contact between this portion of the binding domain and the ligand molecule. 2) The position aligning with Y512 in rOCNC1 is Y in most olfactory channels (the catfish olfactory channel is the only exception, with F) and F in most of the rod or cone photoreceptor channels (Fig. 2). The olfactory channels can be potently activated by both cGMP and cAMP, whereas for photorecep-

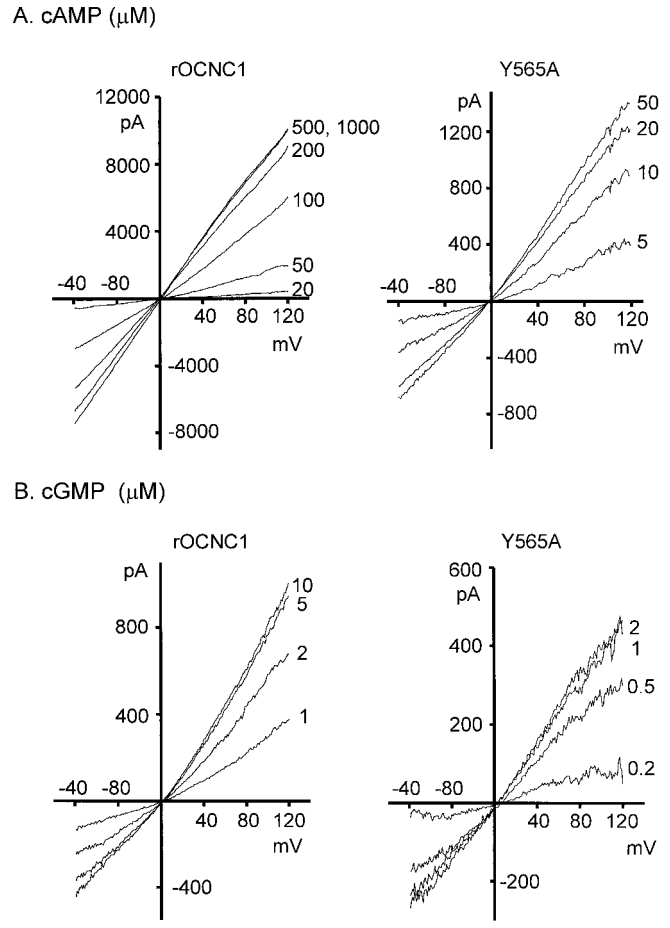

Fig. 5. Representative current-voltage families during voltage ramps from −80 mV to 120 mV of 800-ms duration. Left, rOCNC1; right, rOCNC1-Y565A. A, cAMP. B, cGMP. The basal current recorded in the absence of cyclic nucleotide was subtracted. For wild-type rOCNC1, the basal current comprised almost entirely the leak current at the seal, which was usually 30 to 60 pA at +80 mV. For rOCNC1-Y565A, the basal current was 5 to 30% of maximal current (not shown). This percentage agrees with the single-channel results, where the spontaneous open probability fell into this range (see Fig. 8).

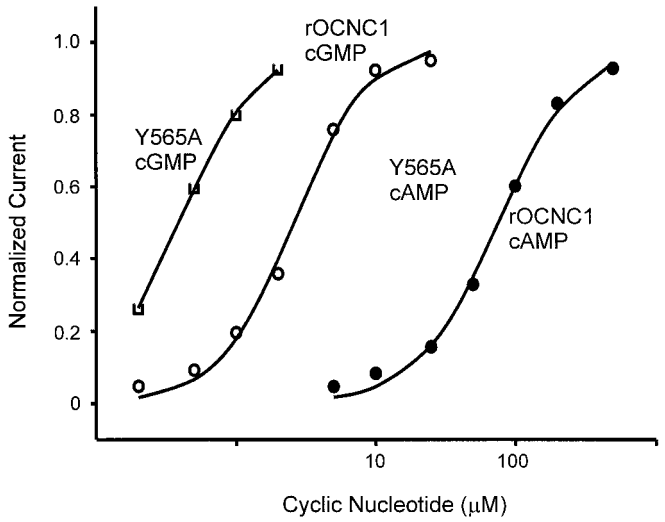

Fig. 6. Dose-response comparison between wild-type rOCNC1 and Y565A at 80 mV. The fitting and normalization were as described in Fig. 3. The horizontal axis is on a logarithmic scale.

tor channels, only cGMP is an effective ligand. This correlation between Y/F identity and agonist specificity raised the possibility that an F at this position in photoreceptor channels contributes to selectivity to cGMP over cAMP. In olfactory channels, if the extra hydroxyl group in tyrosine makes a hydrogen bond with cAMP, but not with cGMP, it could provide stronger affinity or greater efficacy to cAMP, offsetting, if only partially, the selectivity against cAMP displayed by photoreceptor channels. A typical hydrogen bond brings 3 to 7 kcal/mol of free energy difference; at room temperature, 1.36 kcal/mol produces a 10-fold change in an equilibrium constant. Therefore if Y-to-F or F-to-Y mutations add or eliminate one hydrogen bond in either ligand binding or the subsequent conformational changes, a dramatic shift in EC_{50} value is expected.

The actual changes we found were much smaller than 10-fold. Figure 3 compares the dose-response relations for representative recordings from patches expressing rOCNC1 wild-type and Y512F mutant channels, activated by either cAMP or cGMP. Figure 4 shows the comparison between Brcng wild-type and F533Y mutant channels, activated by cGMP. The averaged results from multiple patches are shown in Table 1. The EC_{50} value for cAMP was increased by just over 2-fold in rOCNC1 Y512F, whereas the EC_{50} value for cGMP was unchanged for either mutant. Hill coefficients were unaffected. If the extra hydroxyl group in tyrosine is forming an additional interaction with cAMP, and if this interaction is absent with phenylalanine (as in Brcng) or with cGMP, the potential energy involved is either much less than expected for a typical hydrogen bond or is decreased by compensatory structural changes elsewhere in the protein. Therefore, the strong selectivity for cGMP over cAMP displayed by photoreceptor channels is not likely to be related to the phenylalanine at this position.

To test the involvement of rOCNC1 Y512 in possible hydrophobic interactions, we mutated it to either alanine or serine. These two residues can still participate in hydrophobic clustering, yet they differ in size and polarity and lack the π-electron moiety. The results for Y512A and Y512S of rOCNC1 are summarized in Table 1 and showed very little change from the wild-type channel. Sensitivities for cGMP were unchanged for Y512S, and increased by less than 2-fold for Y512A.

This result, taken by itself, is consistent with the existence of a hydrophobic surface at this region of the tertiary structure. However, when we eliminated hydrophobicity with the Y512D mutation, the apparent sensitivity for either cAMP or cGMP was reduced by only 2-fold (Table 1). The lack of dramatic effect of Y512D therefore argues against a direct hydrophobic contact. The tolerance of a charged side chain

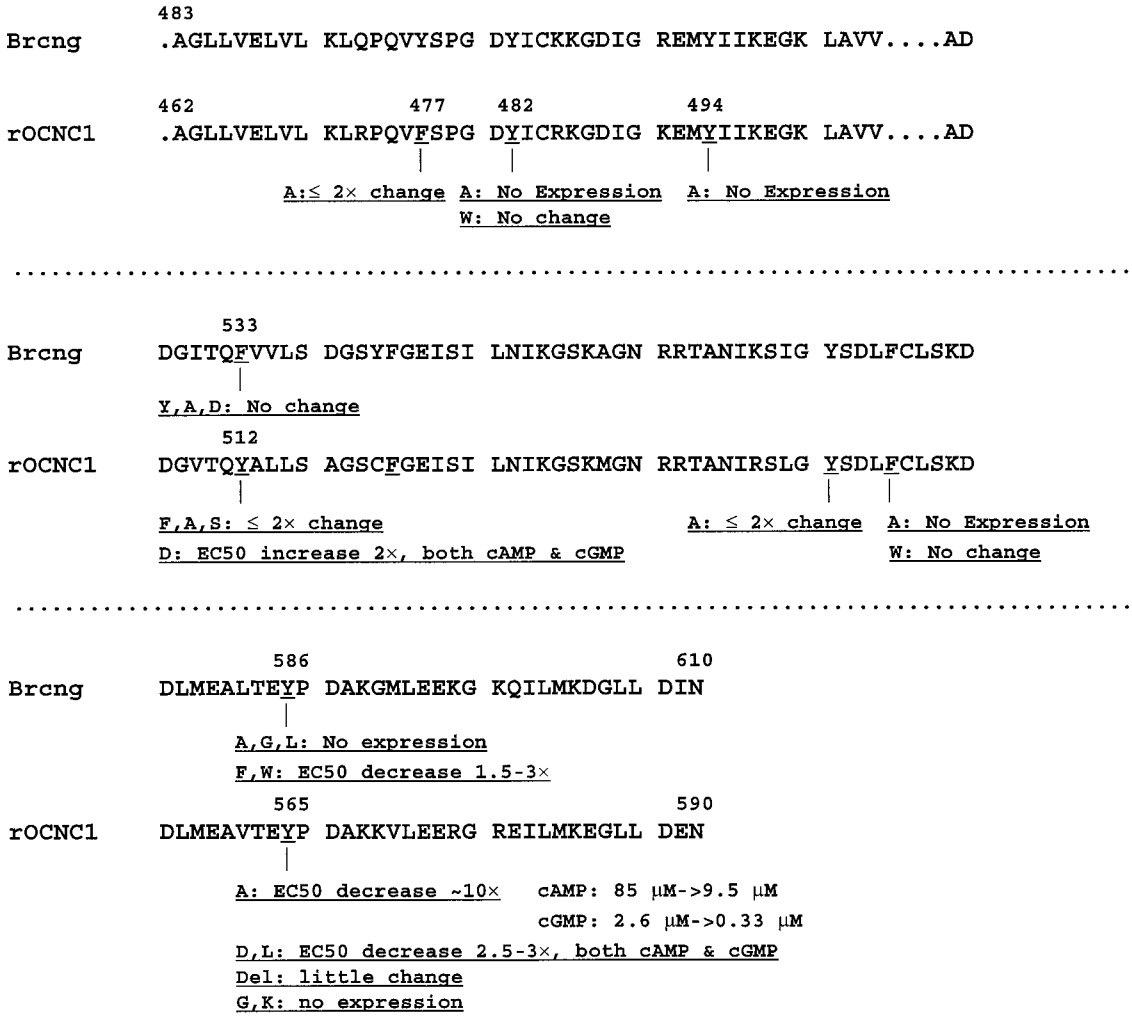

Fig. 7. Summary of mutants made and their major properties.

suggests a polar or charged environment for this portion of the binding domain. Alternatively, two hydrophobic surfaces may have polar intermediates, such as water, between them. The homologous mutations were also made in Brcng. We found that the EC_{50} values for F533A and F533D were indistinguishable from those of the wild-type (Table 1).

In summary, we have found only minor changes in EC_{50} caused by mutation at rOCNC1-Y512 and Brcng-F533, the positions predicted by available structural models to interact strongly with the cyclic nucleotides. Our results indicate that residues at this position are unlikely to form hydrogen bonds or direct hydrophobic interactions with the ligand molecule.

Mutations of Other Aromatic Residues. To examine the functional importance of other aromatic residues in the binding domain, we mutated six additional aromatic residues in the binding-site region of rOCNC1. These were F477, Y482, Y494, Y547, F551, and Y565. Along with Y512, seven of the eight aromatic residues in the rOCNC1 binding domain have been examined. We were unable to generate a mutation for the eighth aromatic residue, F521. The annealed fragments failed to amplify during the "bridge" PCR, and this position was not studied further.

Of the six Y/F-to-A mutations, Y482A, Y494A, and F551A did not express functional channels. The change from an aromatic residue to alanine might be too drastic at these positions. We mutated two of these residues, Y482 and F551, to tryptophan, and found that the mutant channels were similar to the wild-type channel in their properties (Table 1).

Two of the remaining three mutants, F477A and Y547A, expressed channels largely similar to the wild-type channel. Their EC_{50} values differed from those of the wild-type sequence by no more than 2-fold. Aromatic residues at these two positions can be readily replaced by much smaller hydrophobic residues such as alanine; therefore, aromaticity at these two positions is not likely to be essential for channel function.

Y565A, a Hypersensitive Mutant. The last mutation to be described, Y565A, increased the sensitivity for both cAMP and cGMP (Fig. 5). The dose-response relations shown in Fig. 6 and the parameters in Table 1 indicate approximately 10-fold reductions in the EC_{50} value. The major properties of all of the mutations studied were summarized in Fig. 7. Y565A had the same conductance as the wild-type channel (~44 pS at −60 mV, more details below), yet the expression level was reduced by 10- to 30-fold. Single-channel recordings showed 5 to 30% spontaneous opening probabilities (Fig. 8A),

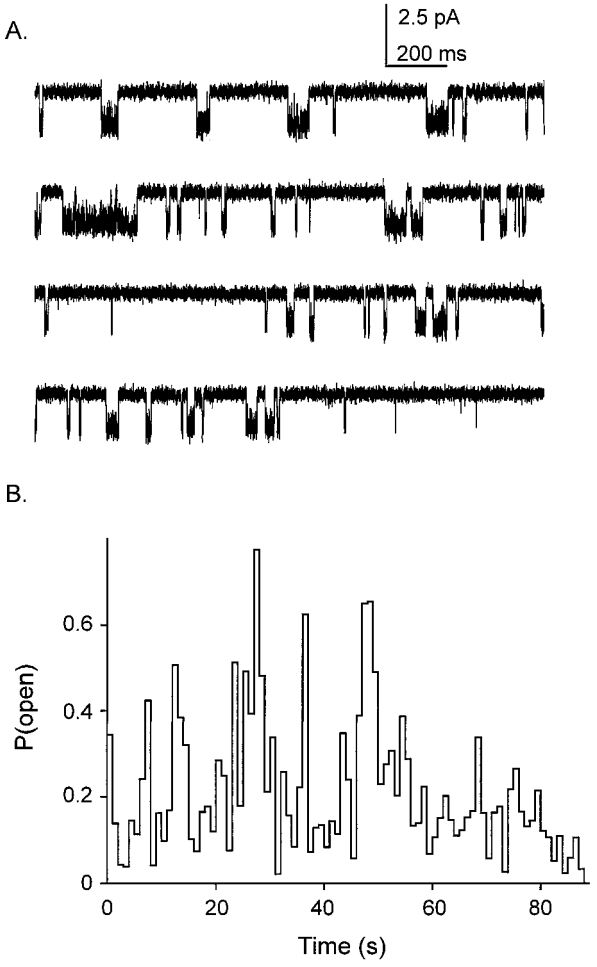

Fig. 8. A, consecutive current traces of a single Y565A channel in the absence of any cyclic nucleotide, recorded at −60 mV. The channel is opening downward. B, the fluctuations of P_{open} during 90 s of spontaneous activity of this channel. The P_{open} values were calculated within 1-s time windows, and the mean ± standard deviation in the total of 90 windows is 21.3 ± 15.9%. Other channels had different P_{open} values, which ranged from 5 to 30%, yet after exposure to cAMP or cGMP, the channels often become sensitized, yielding spontaneous P_{open} values as high as 80%.

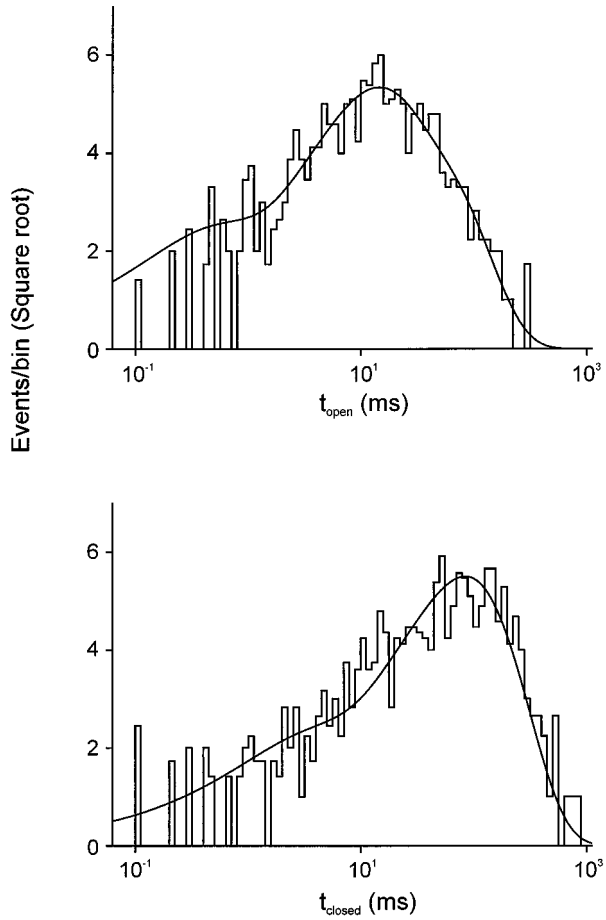

Fig. 9. The open-time (A) and closed-time (B) histograms of the spontaneous openings of the channel shown in Fig. 8. The smooth lines are the fits by sums of exponential functions.

which fluctuated in time (Fig. 8B) and were variable among oocytes both within and across batches. The prominence of spontaneous activities provides a strong indication for facilitated gating transitions in the mutated channels. The open- and closed-time histograms of the spontaneous openings contained multiple components (Fig. 9), indicating complex underlying kinetic states. In the presence of cyclic nucleotides, the maximum open probability was well over 50% and approached 100% in several patches. With increasing concentrations of cAMP, the open times became longer; the closed times became correspondingly briefer (Fig. 10). There was no bursting behavior. In the presence of cyclic nucleotide, there were also fluctuations in P_{open}, which often led to higher sensitivities of the channel. After "sensitization", the channel maintained a high level of activity even after prolonged washing with the ligand-free solution. The parallel mutation in Brcng, Y586A, failed to express. Y586F and Y586W, more conservative mutations, increased cGMP sensitivity by 2-fold and 30%, respectively (Table 1). Apparently, in Brcng, this position is much less tolerant to changes than in rOCNC1.

Changing Y565 of rOCNC1 to L and D gave rise to sensitivities intermediate between wild-type channel and Y565A. Instead of the 10-fold change seen with Y565A, the Y565L and Y565D mutants had ~3-fold higher sensitivities to cAMP and cGMP than the wild-type channel. Evidently, at this position, the size of the side chain matters more than charge or aromaticity. The smaller the residue, the more sensitive the channel, which indicates that an appropriate degree of steric hindrance at this position is important for function.

To test further the effect of size, we made the Y565G mutation. It did not express functionally. We then deleted Y565 in Y565Δ. Interestingly, Y565Δ became much more similar to the wild-type channel than any of the other mutants. The structure of the binding fold does not vary in a linear fashion with the size of the residue at 565; in this case, the deletion was largely compensated for.

Taken together, Y565 in rOCNC1 and Y586 in Brcng are likely to be important determinants of channel function. The primary property that seems to be crucial for their function is the volume of the side chains, rather than the ability to participate in hydrophobic interactions or specific aromatic–aromatic contacts.

Discussion

The homology-based models of binding domains in CNG channel depend heavily on the template structure of CAP and are sensitive to 1) the uncertainties inherent in defining energy terms and 2) the assumptions regarding the intricate and extensive couplings between neighboring side chains. It is therefore important to test these models, particularly the explicit predictions of prominent interactions. In one such experimental test, Thr560 in Brcng was investigated through site-directed mutagenesis and expression (Altenhofen et al., 1991). It was found that Thr560 determined the selectivity of cGMP over cAMP, a finding consistent with the interpretation of an earlier structure model of cGMP-dependent protein kinase (Weber et al., 1989). In another study, Tibbs et al. found that the highly conserved Arg559, one residue upstream of Thr560, formed a favorable ionic bond with cGMP (Tibbs et al., 1998), again agreeing with previous models. The largest shifts caused by amino acid substitutions amounted to 150-fold and 1000-fold differences in EC_{50} values for Thr560 and Arg559, respectively, reflecting free energy differences on the level of 3 to 4 kcal/mol, typical of a hydrogen bond or an ionic pair.

In the present study, however, the changes in EC_{50} value we found with mutations at Y512 of rOCNC1 and F533 of

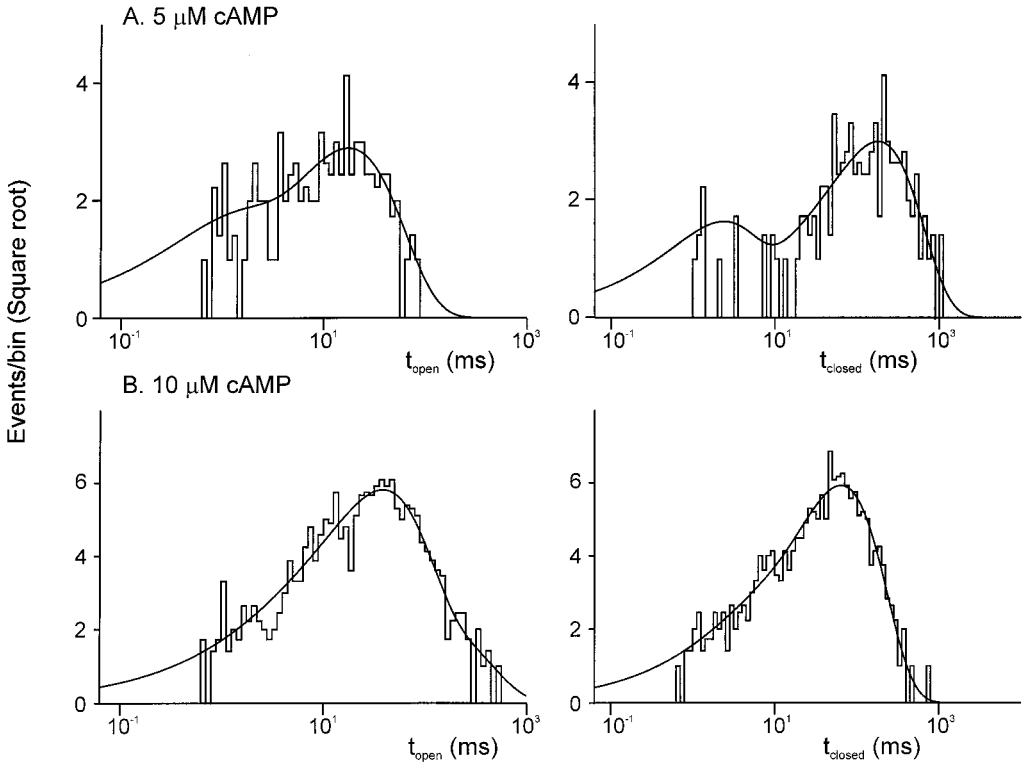

Fig. 10. The open-time (left) and closed-time (right) histograms at two different cAMP concentrations for a Y565A channel other than the one shown in Figs. 8 and 9. A, 5 μM. B, 10 μM. Note that with increasing cAMP, open times were lengthened, whereas the closed times were shortened. The smooth curves were the sum of exponential functions used to fit the observed distributions. The fitting parameters, expressed as time constant (fractional area), are as follows: A, open times, 1 ms (18%) and 18 ms (82%); closed times, 2.1 ms (21%) and 179 ms (79%). B, open times, 4.3 ms (3%), 37 ms (87%), and 128 ms (10%); closed times, 3.8 ms (5%) and 63 ms (95%).

Brcng were much less than expected (Scott et al., 1996). These residues were predicted to interact specifically with cyclic nucleotides and to govern the selectivity of cGMP over cAMP in the photoreceptor channels. Contrary to this prediction, our results indicated that this side chain is unlikely to form a hydrogen bond or direct hydrophobic contact with the ligand molecule in the olfactory channel. Not only is the Y/F difference not important for the higher efficacy of cGMP at the photoreceptor channels, but even the replacement by alanine or glutamate caused no changes appropriate to the free energy for a hydrogen bond or an ion pair. The surprisingly mild effect of introducing a negative charge with glutamate suggested that there is a charged or polar environment for this portion of the binding domain. This result, however, does not rule out hydrophobic interactions mediated by other regions of the binding site.

A recent study showed that the photoaffinity analog of cGMP, 8-(*p*-azidophenacylthio)-[^{32}P]cGMP specifically labels Brcng at V524, V525, and A526, residues that align with β4 in CAP (Brown et al., 1995). This region of the binding site was not noted by the models to interact with the ligand.

The validity of the structural models were further confounded by the uncertainties about the conformation of cAMP and cGMP molecules. These ligands can bind in either the *syn-* or the *anti-* conformation; the two variations lead to profoundly different energetic outcomes. A more definitive examination of related hypotheses would require testing individual combinations of mutant receptors and cyclic nucleotide analogs that have relatively defined preferences for *anti-* or *syn-* conformation.

In the regulatory subunit of PKA, the aromatic–aromatic interactions play an important role in ligand binding. PKA-R1 is one of the many examples of the importance of aromatic residues in ligand recognition, protein folding, and protein conformational changes in general (Hunter, 1994). In a review of 34 high-resolution protein structures, Burley and Petsko (1985) concluded that an average of 60% of aromatic side chains in proteins are involved in aromatic pairs, 80% of which form networks of three or more interacting aromatic side chains. In most common cases, the aromatic rings prefer an edge-to-face configuration and are separated by 4.5 to 7 Å. Nonbonded potential energy calculations indicate that a typical pairwise interaction has a stabilizing energy of −1 to −2 kcal/mol. The conservation of aromatic-aromatic interactions in related proteins is striking, indicating that these interactions play important roles in structure or function. A potassium channel contains crucial edge-to-edge aromatic contacts (Doyle et al., 1998).

The aromatic–aromatic interactions in PRA-R1 are not mediated by residues that align with Leu61 of CAP; instead, the relevant aromatic residues reside in other, unexpected positions (Su et al., 1995). We therefore attempted to examine all of the aromatic residues in the binding domain of rOCNC1 through mutagenesis. At some of these positions, alanine mutations resulted in nonfunctional channels, but tryptophan mutations resulted in responses indistinguishable from those of the wild-type channels. Perhaps channels with reduced function would result from side chains with properties intermediate between alanine and tryptophan. Most of the aromatic-to-alanine mutations that are functional did not result in significant changes in channel properties. However, one mutation, Y565A of rOCNC1, increased agonist sensitivity by 10-fold, indicating that this position is important for channel functioning. Nonetheless, this residue probably does not interact directly with the ligand molecule, for two reasons: 1) the increased spontaneous activity strongly suggests gating changes, and the reduced expression level may result from the desensitization of the constitutively active channels; and 2) assuming that the overall folding pattern is conserved between CAP, PKA-R1,and rOCNC1, this residue would be located between αB and αC, outside the binding pocket. It is also formally possible that Y565 is a site of tyrosine phosphorylation in the wild-type channel (Molokanova et al., 1997).

The αC helix is likely to be mobile during channel activation. In fact, rotation of this helix, either induced or stabilized by the bound ligand molecule, is probably one of the conformational changes that link ligand binding and its ultimate effect, the opening of the pore (Varnum et al., 1995). Y565A is therefore positioned at the "hinge" of the motion. Our data suggest that larger residues at this "pivotal" position favor the closed state of the channel. For instance, after replacement with alanine, we see increased spontaneous activities and an corresponding increase in ligand sensitivity. The fact that Y565A affects cAMP and cGMP to equal extents also argues for a general functional role that is indifferent to the fine structure of the ligand. Residues that interact directly with the ligand probably include D604 in the C helix of Brcng (Varnum et al., 1995).

The distances between the binding pocket, the pore, and Y565 are likely to span a considerable portion of the entire protein, demonstrating the remarkable range of allosteric coupling. The effect of Y565 mutations, particularly the correlation between channel properties and the size of the side chain at this site, place important constraints on future structural models.

Acknowledgements

We thank J. Ho for participating in the early phase of this project. We thank Dr. V. Kumar for the coordinates of the Brcng structural model and Dr. Y. Su for sharing the coordinates of PKA regulatory subunit before publication. We thank Drs. S. Scott and J. Tanaka for exchanging ideas. Dr. William Zagotta provided many stimulating discussions throughout this project.

References

Altenhofen W, Ludwig J, Eismann E, Kraus W, Bonigk W and Kaupp UB (1991). Control of ligand specificity in cyclic nucleotide-gated channels from rod photoreceptors and olfactory epithelium. *Proc Natl Acad Sci USA* **88:**9868–9872.

Brown RL, Gramling R, Bert RJ and Karpen JW (1995) Cyclic GMP contact points within the 63-kDa subunit and a 240-kDa associated protein of retinal rod cGMP-activated channels. *Biochemistry* **34:**8365–8370.

Bubis J and Taylor SS (1987) Limited proteolysis alters the photoaffinity labeling of adenosine 3′,5′-monophosphate dependent protein kinase II with 8-azidoadenosine 3′,5′-monophosphate. *Biochemistry* **26:**5997–6004.

Burley SK and Petsko GA (1985) Aromatic-aromatic interaction: a mechanism of protein structure stabilization. *Science (Washington DC)* **229:**23–28.

Doyle D, Cabral J. M., Pfuetzner R, Kuo A, Gulbis J, Cohen S, Chait B and MacKinnon R (1998) The structure of the potassium channel: molecular basis of K^+ conduction and selectivity. *Science (Washington DC)* **280:**69–77

Dhallan RS, Yau KW, Schrader KA and Reed RR (1990) Primary structure and functional expression of a cyclic nucleotide-activated channel from olfactory neurons. *Nature (Lond)* **347:**184–187.

Fesenko EE, Kolesnikov SS and Lyubarsky AL (1985) Induction by cyclic GMP of cationic conductance in plasma membrane of retinal rod outer segment. *Nature (Lond)* **313:**310–313.

Gordon S and Zagotta W (1995) A histidine residue associated with the gate of the cyclic nucleotide-activated channels in rod photoreceptors. *Neuron* **14:**177–183.

Higuchi, R (1990) Recombinant PCR, in *PCR Protocols: A Guide to Methods and Applications* (Innis MA, Gelfand DH, Sninsky JJ and White TJ eds) pp 177–183, Academic Press, Inc., San Diego.

Hunter CA (1994) Meldola lecture: The role of aromatic interactions in molecular recognition. *Chem Soc Rev* **23:**101–109.
Jan LY and Jan YN (1990) A superfamily of ion channels. *Nature (Lond)* **345:**672.
Kaupp UB, Niidome T, Tanabe T, Terada S, Bönigk W, Stühmer W, Cook NJ, Kangawa K, Matsuo H, Hirose T, Miyata T and Numa S (1989) Primary structure and functional expression from complementary DNA of the rod photoreceptor cyclic cGMP-gated channel. *Nature (Lond)* **342:**762–766.
Kumar VD and Weber IT (1992) Molecular model of the cyclic GMP-binding domain of the cyclic GMP-gated ion channel. *Biochemistry* **31:**4643–4649.
Li J, Zagotta WN and Lester HA (1997) Cyclic nucleotide-gated channels: structural basis of ligand efficacy and allosteric modulation. *Q Rev Biophys* **30:**177–193.
Liman ER, Tytgat J and Hess P (1992) Subunit Stoichiometry of a Mammalian K+ Channel Determined by construction of multimeric cDNAs. *Neuron* **9:**861–871.
McKay DB and Steitz TA (1981) Structure of catabolite gene activator protein at 2.9 Å resolution suggests binding to left-handed B-DNA. *Nature (Lond)* **290:**744–749.
Molokanova E, Trivedi B, Savchenko A and Kramer RH (1997) Modulation of rod photoreceptor cyclic nucleotide-gated channels by tyrosine phosphorylation. *J Neurosci* **17:**9068–9076.
Nakamura T and Gold GH (1987) A cyclic nucleotide-gated conductance in olfactory receptor cilia. *Nature (Lond)* **325:**442–444.
Quick MW, Naeve J, Davidson N and Lester HA (1992) Incubation with horse serum increases viability and decreases background GABA transport in *Xenopus* oocytes. *Biotechniques* **13:**358–362.
Scott SP, Harrison RW, Weber IT and Tanaka JC (1996) Predicted ligand interactions for 3′5′-cyclic nucleotide gated channel binding sites: comparison of retina and olfactory binding site models. *Protein Eng* **9:**333–344.
Shabb J and Corbin JD (1992) Cyclic nucleotide-binding domains in proteins having diverse functions. *J Biol Chem* **267:**5723–5726.
Sigworth FJ and Sine SM (1987) Data transformations for improved display and fitting of single-channel dwell time histograms. *Biophys J* **52:**1047–1054.
Su Y, Dostmann WR, Herberg FW, Durick K, Xuong NH, Ten Eyck L, Taylor SS, Varughese KI (1995) Regulatory subunit of protein kinase A: structure of deletion mutant with cAMP binding domains. *Science (Washington DC)* **269:**807–813.
Tibbs GR, Liu DT, Leypold BG and Siegelbaum SA (1998) A state-independent interaction between ligand and a conserved arginine residue in cyclic nucleotide-gated channels reveals a functional polarity of the cyclic nucleotide binding site. *J Biol Chem* **273:**4497–4505.
Varnum MD, Black KD and Zagotta WN (1995) Molecular mechanism for ligand discrimination of cyclic nucleotide-gated channels. *Neuron* **15:**619–625.
Weber IT, Shabb JB and Corbin JD (1989) Predicted structures of the cGMP binding domains of the cGMP-dependent protein kinase: A key alanine/threonine difference in evolutionary divergence of cAMP and cGMP binding sites. *Biochemistry* **28:**6122–6127.
Weber IT and Steitz TA (1987) Structure of a complex of catabolite gene activator protein and cyclic AMP refined at 2.5 Å resolution. *J Mol Biol* **198:**311–326.
Yau K-W and Baylor DA (1989) Cyclic GMP-activated conductance of retinal photoreceptor cells. *Annu Rev Neurosci* **12:**289–327.
Zufall F, Firestein S and Shepherd GM (1994) Cyclic nucleotide-gated ion channels and sensory transduction in olfactory receptor neurons. *Annu Rev Biophys Biomol Struct* **23:**577–607.

Send reprint requests to: Dr. Henry A. Lester, Division of Biology, 156-29, California Institute of Technology, Pasadena, CA 91125. E-mail: lester@caltech.edu